RSC Advances

PAPER

View Article Online
View Journal | View Issue

Open Access Article. Published on 12 March 2026. Downloaded on 3/19/2026 3:27:56 PM.
This article is licensed under a Creative Commons Attribution-NonCommercial 3.0 Unported Licence.

Check for updates

Cite this: *RSC Adv.*, 2026, **16**, 13774

Simultaneous detection of thyroid-stimulating hormone and C-reactive protein using a multiplex lateral flow device for improved hypothyroidism diagnosis

Sara E. McNamee, *[a] Santosh Kumar Bikkarolla,[a] Kerry-Louise Skillen,[a] Deepesh Upadhyay,[b] Mary Jo Kurth,[b] Peter Fitzgerald[b] and James McLaughlin[a]

Received 19th January 2026
Accepted 24th February 2026

DOI: 10.1039/d6ra00470a

rsc.li/rsc-advances

The clinical and medical industries require practical and cost-effective solutions for simultaneous biomarker determination to replace time-consuming conventional testing methods. Hypothyroidism, or an underactive thyroid, occurs when your thyroid gland doesn't make enough thyroid hormones to meet your body's needs. Over time, hypothyroidism that isn't treated can lead to other health problems, such as high cholesterol and heart problems. This study introduces a novel, rapid, easy to use and portable multiplex lateral flow device (LFD) designed for the simultaneous detection of Thyroid stimulating hormone (TSH) and C-reactive protein (CRP) in human serum to aid in diagnosing hypothyroidism. Designed to meet the clinical need for hypothyroidism as well as rapid, cost-effective screening tools, the multiplex LFD delivers quantitative results within 30 minutes, showing detection limits of 2.1 μIU ml^{-1} for TSH and 0.007 μg ml^{-1} for CRP. Preliminary performance using 17 certified serum samples demonstrated a 60–130% recovery rate. The results demonstrate the proof of concept and preliminary performance of the multiplex LFD, positioning this LFD as a significant advancement in the field of point of care (POC) diagnostics for hypothyroidism.

1 Introduction

POC testing is defined as a diagnostic test that is performed at or near to the site of the patient with the result leading to a potential change in the care of that patient. POC tests provide results in real time, rather than in hours or days, allowing faster and better decisions about medical care. Essentially POC testing can offer a rapid turnaround time, with an immediate impact on patient care and treatment. For some conditions, like diabetes, POC testing has already drastically altered how care is delivered and managed. Efforts have been underway to develop new technologies for more sensitive and specific POC tests. Recent reviews on POC testing considered nanoparticles,[1] artificial intelligence,[2] smartphones[3] and reader technologies.[4] With the market for POC testing only expected to expand, it will continue to change the way healthcare is delivered.

An LFD is an inexpensive simple device that can be used in POC testing. LFDs can be used to test for a target analyte in a sample without requiring the use of specialised or expensive equipment. They are simple to use, disposable and can test for biomarkers in samples such as saliva, blood or urine. They therefore satisfy the "ASSURED" World Health Organization (WHO) benchmark of POC tests. This means they are affordable, sensitive, specific, user-friendly, rapid and robust, equipment-free and deliverable, making them ideal for healthcare facilities. An LFD is made up of a sample pad, a conjugate pad, a nitrocellulose membrane (that contains test and control lines) and an absorbent pad. The principle behind the LFD is simple, a liquid sample, containing the analyte of interest, moves by capillary force through various zones of the LFD, on which molecules that can interact with the analyte are attached. The read-out, represented by the lines appearing can be assessed by eye or using an LFD reader. Several reviews are available providing overviews of the latest research involving the use of LFDs for qualitative and quantitative analysis, summarising the accomplishments, weaknesses and future challenges in this area.[5–7] Theoretical studies on LFDs focus on understanding the underlying physical, chemical and biological mechanisms to optimise their diagnostic accuracy, particularly regarding sensitivity and specificity. There are several key papers on the mechanisms of LFDs that investigate the intersection of fluid dynamics, reaction kinetics and nanomaterial engineering to improve diagnostic performance in the literature.[8–12] These studies suggest that strategic optimisation

[a]*Nanotechnology and Integrated Bioengineering Centre (NIBEC), School of Engineering, University of Ulster, 2-24 York Street, Belfast, BT15 1AP, UK*
[b]*Randox Laboratories Ltd, 55 Diamond Road, Crumlin, County Antrim, BT29 4QY, UK.*
E-mail: se.mcnamee@ulster.ac.uk

© 2026 The Author(s). Published by the Royal Society of Chemistry

Open Access Article. Published on 12 March 2026. Downloaded on 3/19/2026 3:27:56 PM. This article is licensed under a Creative Commons Attribution-NonCommercial 3.0 Unported Licence.

of gold nanoparticles, antibodies on the test line and flow rate can significantly enhance sensitivity.

There is a growing requirement in POC diagnostics for the generation of tests that can detect more than one analyte in a single device. In recent years innovative nanoscience and technology with state-of-the-art sensing equipment has allowed the emergence of novel detection platforms. The emergence of multiplex diagnostics has become a unique and important tool for high-throughput analysis providing promising methods in which several targets are detected simultaneously by LFD.[9–16] Multiplexing, however, does not come without its constraints with non-specific binding, antibody cross reactivity, and low sensitivity all being common issues encountered. Effort is, therefore, focused on the development of novel, rapid, inexpensive, user friendly, sensitive and cost-effective multiplex detection methods. The simultaneous identification of several targets in one single test, reducing time and costs per analysis is a most attractive option. In a standard LFD configuration, multiple test lines can be dispensed in a multiplex LFD. However, there is a limit on the number of lines that can be dispensed before lines start to merge which lowers the sensitivity of the assay resulting in false positives. These issues can be overcome by using LFDs with spotted microarrays instead of lines. The key advantages of the spotted microarray over traditional lines include the elimination of lines merging, reduced false positives and therefore increased specificity, high density multiplexing and improved quantitative data. This research focuses on the use of a spotted microarray to develop a multiplex LFD for two biomarkers – TSH and CRP with the added possibility of adding more biomarkers to the panel in the future to cover a complete thyroid check. Additionally, the evolution of diagnostic tools such as microarrays are novel and provide actionable clinical insights and open the possibility of personalised medicine.

TSH, also known as thyrotropin or thyrotrophin, is a hormone that controls the way other hormone's function. Basically, it stimulates the production of two main hormones, thyroxine (T4) and triiodothyronine (T3). In a complex and elegant system, the pituitary gland, hypothalamus and thyroid gland all work together. Without TSH, the whole system can't properly function. A normal reference range for TSH levels is between 0.5 to 5.0 μIU ml^{-1} as reported by the American Thyroid Association, however, normal may look different for each patient. Generally, if TSH is <0.5 μIU ml^{-1}, the thyroid gland is overactive (hyperthyroidism) and anything >5.0 μIU ml^{-1}, the thyroid gland is underactive (hypothyroidism). There are several commercial LFDs available for TSH and diagnosis of hypothyroidism (Sterilab Services, Personal Diagnostics and BTNX Inc.). Several interesting and innovative TSH LFDs are also described in the literature.[17–20] A recent review by Khelifa *et al.* provides an overview of recent advances for the detection of hormone biomarkers including TSH by LFD.[21]

CRP is produced in the liver in response to inflammation. Normally, levels of CRP are low in your blood. Moderately to severely elevated levels may be a sign of a serious infection or other inflammatory condition. However, a CRP test alone does not explain the cause or location of the inflammation meaning that the CRP test is an extremely non-specific test. Providers, therefore, will generally order additional tests if the CRP results demonstrate inflammation. Ridker proposed thresholds of CRP for the risk of cardiovascular diseases as follows: <1 mg L^{-1} CRP is a low risk, 1–3 mg L^{-1} is moderate risk and a high risk occurs when CRP >3 mg L^{-1}.[22] There are several commercial LFDs available for CRP (Sterilab Services, Biopanda, Alpha Labs and BTNX Inc.) and several interesting and innovative CRP LFDs are detailed in the literature.[23–28]

TSH is used to diagnose thyroid disorders in conjunction with T3 and T4. CRP is not a routine investigation parameter to diagnose thyroid disorders, although many thyroid conditions involve inflammation. Christ-Crain *et al.* first reported increased CRP in patients with overt hypothyroidism or subclinical hypothyroidism citing it as an additional risk factor for development of coronary heart disease in those patients.[29] Tuzcu *et al.* found the mean value of CRP in thyroid patients was 4.2 ± 0.8 mg L^{-1} compared to 1.05 ± 0.3 mg L^{-1} in the control group.[30] A study by Nagasaki *et al.* found that the baseline CRP level was significantly higher in hypothyroid patients than in normal controls.[31] Savas *et al.* concluded that there were significant changes in the level of inflammatory markers in patients with thyroid disorders.[32] A study conducted by Ahmad *et al.* found a positive correlation between TSH and CRP, they found the mean CRP was 3.06 ± 0.07 mg L^{-1} in thyroid patients compared to 0.88 ± 0.075 mg L^{-1} in controls and concluded that abnormal thyroid hormones level interferes with the serum levels of CRP which can have the implications related to cardiovascular diseases.[33] Tang *et al.* found that CRP and TSH were risk factors for hypothyroidism suggesting that thyroid functions should be monitored closely for the early detection of hypothyroidism.[34] In summary, there appears to be a clear association between CRP, TSH and hypothyroidism suggesting the need for monitoring both TSH and CRP levels in hypothyroidism patients. The aim of this research was to demonstrate the proof of concept and feasibility of a multiplex LFD for the simultaneous detection of two biomarkers for hypothyroidism and to assess the performance of serum samples in a preliminary study.

2. Experimental

2.1. Chemicals, reagents and materials

Phosphate buffered saline (PBS) tablets, tween 20, bovine serum albumin (BSA), sucrose, *N*-(3-dimethylaminopropyl)-*N*′-ethylcarbodiimide hydrochloride (EDC), tris buffered saline (TBS), 4-morpholineethanesulfonic acid (MES) and hydroxylamine were purchased from Sigma-Aldrich (UK). Gold-carboxyl conjugation kit (40 nm) and sulfo-*N*-hydroxysuccinimide (NHS) were purchased from Abcam (UK). Monoclonal antibodies for CRP and TSH, CRP standard and CRP free serum were purchased from Fitzgerald Industries International (USA). Goat anti-mouse IgG was purchased from Thermofisher (UK). TSH standard was purchased from The National Institute for Biological Standards and Control (NIBSC, UK). Conjugate pad (8951) and absorbent pad (A270) were purchased from Ahlstrom (Finland). Nitrocellulose membrane (CN140) was purchased from Sartorius

Open Access Article. Published on 12 March 2026. Downloaded on 3/19/2026 3:27:56 PM.
This article is licensed under a Creative Commons Attribution-NonCommercial 3.0 Unported Licence.

(Germany). Sample pad (FRI (0.6)) was purchased from MDI Membrane Technologies (India). Backing card was purchased from Lohmann Technologies (UK). TSH free serum was purchased from H2B (France). Certified CRP serum samples were purchased from Lampire Biological Laboratories (USA) and certified TSH samples were purchased from TCS Biosciences (UK).

2.2. Instrumentation

A Sciflexarrayer S3 (Scienion, Germany) was used for printing antibody microarrays. A ZX1010 dispense system (Biodot, UK) was used for spraying gold nanoparticles. A Leelu LFD reader (Lumos Diagnostics, USA) was used for capturing LFD images.

2.3. Conjugation of gold nanoparticles with detection antibodies

Monoclonal antibodies were covalently attached to 40 nm gold nanoparticles using a gold conjugation kit following the manufacturer's instructions. The gold conjugation has been characterised in previous research by UV-VIS and TEM.[19] In brief, Gold-NPs (50 μl), antibody (20 μl), EDC (20 μl, 1 mM) and MES buffer (10 μl, 100 mM, pH 5.0) were mixed and incubated for 30 min. TBS buffer (1 ml, containing 0.05% tween) was added to the mixture and centrifuged at 10 000 rpm for 10 min at 20 °C. The supernatant was carefully removed and the pellet of Gold-Ab-NP were resuspended in TBS buffer (90 μl, containing 0.05% tween and 0.5% BSA) to obtain optical density (OD) 20. A slight alteration of the conjugation method described was followed for the Gold-TSH-NP. Gold-NPs (50 μl), TSH antibody (20 μl), EDC (20 μl, 1 mM), NHS (40 μl, 1 mM) and MES buffer (10 μl, 150 mM, pH 5.0) were mixed and incubated for 30 min. To stop the reaction, hydroxylamine (0.5 μl) was added to the solution and incubated for 10 min at room temperature on a roller. TBS buffer (1 ml, containing 0.05% tween) was added to the mixture and centrifuged at 10 000 rpm for 10 min at 20 °C. The supernatant was carefully removed and the pellet of Gold-TSH-NP were resuspended in TBS buffer (90 μl, containing 0.05% tween and 0.5% BSA) to obtain OD 20. For spraying onto conjugate pads, the final step of the conjugation for both CRP and TSH was omitted. Instead, the Gold-NPs were resuspended in 390 μl of gold drying buffer (2% BSA, 1% tween and 5% sucrose) to obtain OD 5. Gold-CRP-NP and Gold-TSH-NP were mixed 1 : 1 and the Gold–NP mixture was sprayed onto a glass fibre conjugate pad (17 mm) at a flow rate of 20 μl cm^{-1} using the AirJet dispenser on the Biodot XZ1010. The sprayed conjugate pad was dried in an oven at 37 °C for 120 min. Finally, the sprayed conjugate pad was stored in sealed aluminum foil bags with desiccant until further processing.

2.4. Microarray design and immobilisation of capture antibodies

The microarray design was developed as a sandwich assay using two pairs of monoclonal antibodies for CRP and TSH. TSH capture antibody, CRP capture antibody and goat anti-mouse IgG (control antibody) were diluted in printing buffer (10 mM phosphate buffer pH 7.4 and 1% sucrose) at a concentration of 1 mg ml^{-1}. TSH antibody (×3 replicates), CRP antibody (×3 replicates), goat anti-mouse IgG (×3 replicates) and corner guide spots (goat anti-mouse IgG, ×4 replicates) were printed on nitrocellulose membrane (25 mm) with 10 nl spots using a Sciflexarrayer S3 in a 23 × 9 microarray layout (Fig. 1). Corner guide spots were used only for data processing downstream. The printed nitrocellulose membrane was dried in an oven at 37 °C for 60 min and stored in sealed aluminum foil bags with desiccant until further processing.

2.5. LFD configuration, lamination and assembly

The multiplex LFD design and configuration consisting of sample pad (10 mm), conjugate pad (17 mm), nitrocellulose membrane (25 mm) and absorbent pad (20 mm) with the components of the strip fixed to a backing card (60 mm) (Fig. 2). Sample is deposited on the sample pad and migrates towards the conjugate pad. The Gold-NP conjugated antibodies bind the target biomarker and migrate to the test spots on the nitrocellulose membrane, where the bound target biomarker is captured. The LFD materials were laminated onto a plastic backing card with an overlap of 5 mm between the materials and cut into 5 mm LFD strips. LFDs were assembled as either a half LFD (nitrocellulose membrane and absorbent pad only) or full LFD (nitrocellulose membrane, conjugate pad, sample pad and absorbent pad). Half LFDs were used predominately during the optimisation stages to speed up the optimisation process and full LFDs were used during the final characterisation stages.

2.6. LFD assay procedure

Two LFD assays were employed depending on the LFD layout *e.g.*, half LFD (wet assay) or full LFD (dry assay). The volume of running buffer varied depending on the parameter being assessed with the total volume generally being approximately 120 μl to allow adequate wicking of sample through LFD materials. Sample (50 μl), Gold-CRP-NP (5 μl, OD 5), Gold-TSH-NP (5 μl, OD 5) and running buffer (60 μl, 10 mM PBS, 2% BSA and 0.1% tween) were incubated with a half LFD for 30 min. Sample (50 μl) and running buffer (70 μl, 10 mM PBS, 2% BSA and 0.1% tween) were incubated with a full LFD for 30 min.

2.7. LFD optimisation

The optimisation process included choosing the appropriate antibody pair, printing parameters, gold conjugation conditions and LFD materials. These parameters were assessed to give the best performance of the final LFD in terms of sensitivity, dynamic range and overall performance.

2.8. LFD characterisation

LFD characterisation included examining limit of detection (LOD), single and multiplex analysis and matrix effects. For each characterisation experiment eight-point calibration curves for TSH and CRP were prepared in PBS or serum. Each calibrant was assessed in duplicate ($n = 2$ LFDs, $n = 3$ spots per LFD).

 © 2026 The Author(s). Published by the Royal Society of Chemistry

Open Access Article. Published on 12 March 2026. Downloaded on 3/19/2026 3:27:56 PM.
This article is licensed under a Creative Commons Attribution-NonCommercial 3.0 Unported Licence.

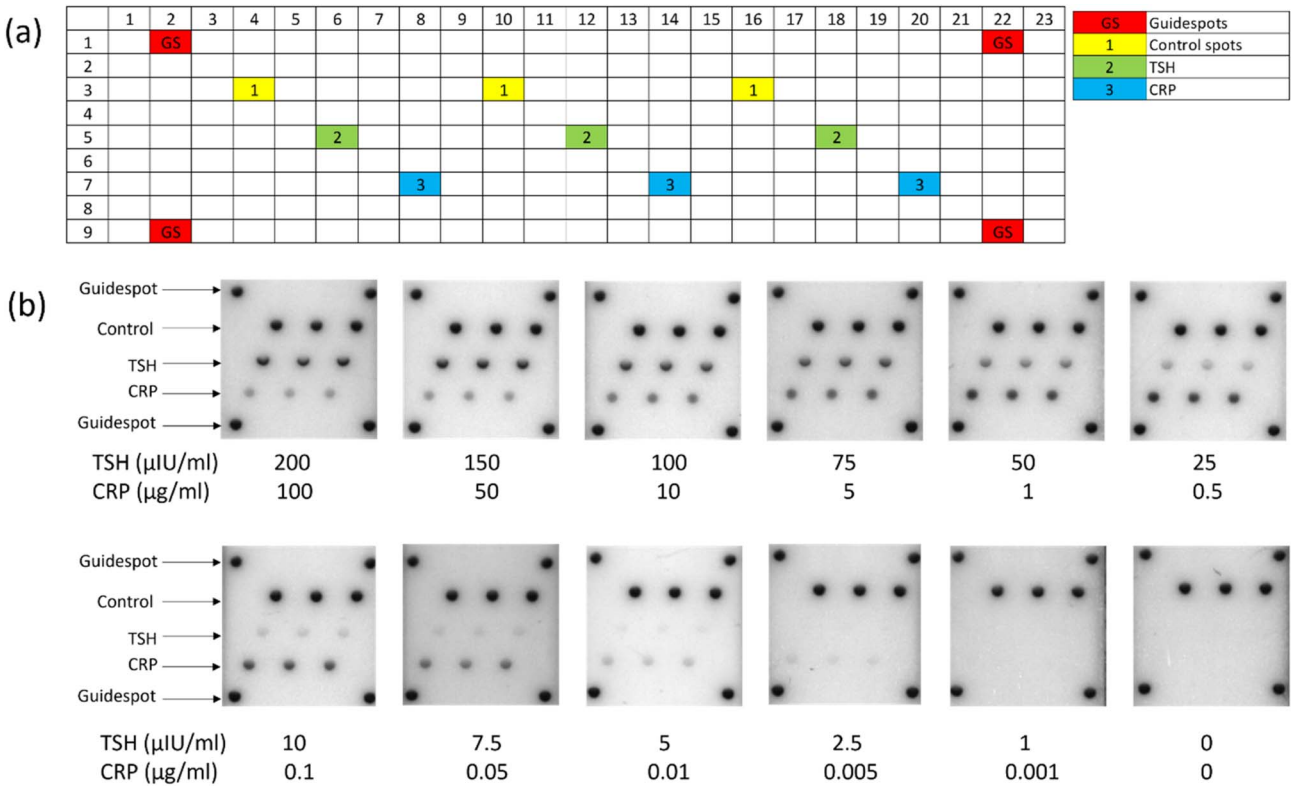

Fig. 1 (a) Multiplex LFD microarray layout including TSH antibody (×3 replicates), CRP antibody (×3 replicates), goat anti-mouse IgG (×3 replicates) and corner guide spots (goat anti-mouse IgG, ×4 replicates) printed using a Sciflexarrayer S3 in a 23 × 9 microarray layout. (b) Images captured using the Leelu LFD reader (Lumos Diagnostics) for a 12-point multiplex calibration curve for both TSH and CRP. Images are inverted by the Leelu LFD reader.

2.9. Limit of dectection

The LOD for this research was determined as the IC_{10} (the concentration providing a 10% inhibition of the signal) of the calibration curve and was interpolated from the four-parameter logistic (4PL) function. A visual LOD was also determined and was defined as the concentration of biomarker providing a test spot signal visible by the Lumos Leelu LFD reader after image processing.

2.10. Analysis of clinical serum samples

Real certified incurred serum samples were also assessed in a preliminary study. The certified incurred serum samples were assessed singly but read from a duplicate serum calibration curve. This was to replicate real-world application as real samples would only be tested by one LFD. Certified serum samples ($n = 17$) including TSH negative ($n = 1$), TSH positive ($n = 12$) and CRP positive ($n = 4$) were analysed by the optimised multiplex LFD. Certified samples were read from a single serum calibration curve due to issues sourcing a TSH and CRP free serum. The sample concentrations for the certified samples were interpolated from a 4PL calibration curve using GraphPad Prism 10.6.1 (GraphPad Software, USA). Results were compared to those obtained by the supplier.

2.11. Image analysis and data processing

LFDs were read by the Leelu LFD reader and images were manually processed using ImageJ (version 1.53 t). All analysis was performed in duplicate unless otherwise stated. The mean, SD and % CV were calculated per LFD ($n = 3$ spots) and per duplicate LFD analysis ($n = 2$ LFDs). Calibration curves were constructed by plotting the grayscale intensities as determined by ImageJ against the logarithm concentrations of the biomarkers. A 4PL regression model was plotted using GraphPad Prism 10.6.1 (GraphPad Software, USA). Displayed error bars represent the standard deviation (SD) of the mean intensities.

3. Results and discussion

The present study outlines the use of this technology to detect two biomarkers in serum for hypothyroidism in a multiplex LFD format (Fig. 1 and 2). The increasing concerns in relation to both health and treatment plans have necessitated the need for rapid, sensitive, portable, high throughput and multiplex detection systems.

3.1. LFD optimisation

The optimisation process included choosing the appropriate antibody pair, printing parameters, gold conjugation

Open Access Article. Published on 12 March 2026. Downloaded on 3/19/2026 3:27:56 PM.
This article is licensed under a Creative Commons Attribution-NonCommercial 3.0 Unported Licence.

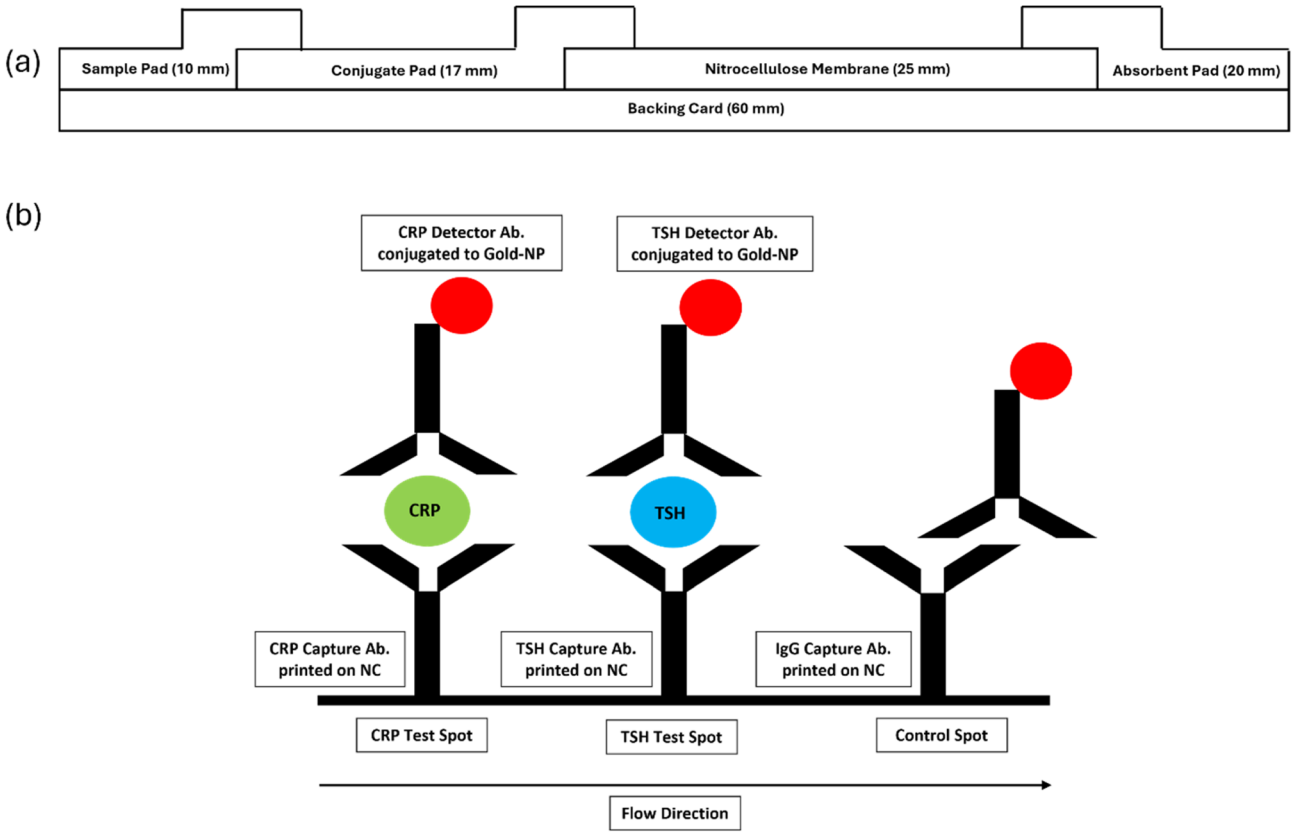

Fig. 2 (a) Schematic representation of the multiplex LFD design and configuration consisting of sample pad (10 mm), conjugate pad (17 mm), nitrocellulose membrane (25 mm) and absorbent pad (20 mm). The components of the strip are fixed to a backing card (60 mm). (b) Schematic representation of the multiplex LFD mechanism. Sample is deposited on the sample pad and migrates towards the conjugate pad. The Gold-NP conjugated antibodies bind the target biomarker and migrate to the test spots on the nitrocellulose membrane, where the bound target biomarker is captured.

conditions and LFD materials to give the best performance of the final LFD in terms of sensitivity, dynamic range and overall performance. At each optimisation step the number of possible combinations was reduced and the LFD was built layer by layer. Unfortunately, the development process was not linear and after each stage of optimisation, the preceding stages often needed to be revisited and reoptimised. Several microarray designs were trialled with the final LFD microarray layout consisting of a 23 × 9 design with a staggered spatial layout for each spot. This layout allowed each spot and replicate to have its own flow pathway along the LFD and thus mitigating the risk of non-specific binding. Additionally, an important factor to remember when developing a truly multiplex assay is that compromises must be made for one biomarker to the potential detriment of another biomarker. During the optimisation stages this was very evident as the two biomarkers chosen in this study came with their own constraints. Several different antibody suppliers and antibody pairs were initially examined to determine the optimum antibody pair for each biomarker. In the end the best antibodies were chosen, although not ideal, it was beyond the scope of this study to continue characterising antibodies. Instead, it was decided that the optimisation process would continue with what was currently showing the best performance with the hope that during optimisation the final performance could be improved. It was evident that for CRP hook effect was observed and for TSH sensitivity was low. Therefore, the printing and gold conjugation for both biomarkers were optimised considering these parameters. Hook effect is a phenomenon whereby the effectiveness of antibody binding is impaired when there is too much antibody or antigen present. The formation of immune complexes stops increasing as analyte increases. Instead, a decrease is observed producing a hook shape on the graph. Hook effect will ultimately limit the dynamic range of the assay and prevent accurate quantification. Several methods were therefore trialled to mitigate hook effect for CRP. These included altering printing (antibody spotting concentration, spotting volume) and gold conjugation (antibody to Gold-NP concentration, Gold-NP OD, gold OD volume) parameters. Sample volume appeared to have the most significant effect on hook effect for CRP. Sample volumes of 1, 2.5, 5, 10, 25 and 50 μl were assessed to determine optimum sample volume (Fig. 3) in regard to LOD, hook effect and best overall LFD performance. Table 1 shows the LOD based on IC_{10} and visual LOD for each sample volume assessed for TSH and CRP. LOD for TSH was 1.5 μIU ml^{-1} with a corresponding visual LOD of 2.5 μIU ml^{-1} using a 50 μl sample

 © 2026 The Author(s). Published by the Royal Society of Chemistry

Open Access Article. Published on 12 March 2026. Downloaded on 3/19/2026 3:27:56 PM.
This article is licensed under a Creative Commons Attribution-NonCommercial 3.0 Unported Licence.

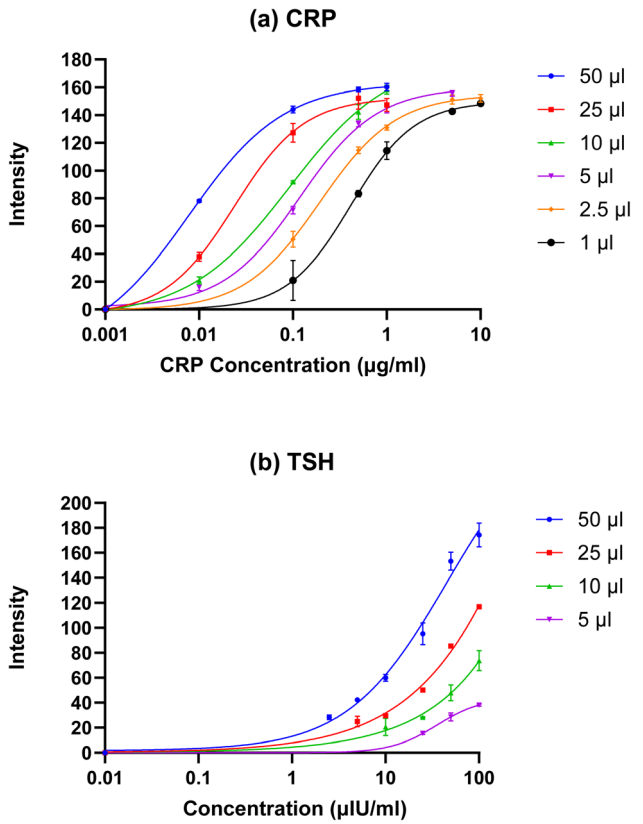

Fig. 3 Sample volume assessment for (a) CRP and (b) TSH using the multiplex LFD ($n = 2$ LFDs, $n = 3$ spots per LFD). Sample volumes of 2.5 µl and 1 µl were also assessed for TSH but could not be plotted as a 4PL fit calibration curve due to low sensitivity and missing calibration points on the curves.

volume. This compared to a LOD of 9.7 µIU ml^{-1} (5 µl) and visual LOD of 50 µIU ml^{-1} (1 µl) using lower sample volumes. LOD for CRP was less affected by sample volume with a LOD of 0.002–0.075 µg ml^{-1} (50–1 µl). The visual LOD for CRP was 0.01 µg ml^{-1} (50, 25, 10 and 5 µl sample volume) and 0.1 µg ml^{-1} (2.5 and 1 µl sample volume). Sample volume, however, had the most significant effect on hook effect for CRP. Hook effect was mitigated from 1 µg ml^{-1} to 50 µg ml^{-1} simply by decreasing the sample volume from 50 µl to 1 µl. To meet clinical requirements for diagnosing hypothyroidism, a sample volume of 50 µl was selected to ensure the necessary sensitivity for TSH detection. An alternative LFD assay was assessed so that hook effect could be mitigated for CRP while maintaining sensitivity for TSH. This assay was completed in three steps with a total incubation time of 60 min and. Briefly the sample was added to the LFD, followed by a wash step and finally the Gold-NP were added in a liquid format. Incorporating this time delay and wash assay for CRP did help to mitigate hook effect but it did not improve the dynamic range of the assay. Instead, intensity plateaued from 1–10 µg ml^{-1} meaning that the assay could only report >1 µg ml^{-1} at these intensity ranges and would not give accurate concentration quantification. Interestingly this assay format showed significant suppression of intensity for TSH and a loss of sensitivity to 5 µIU ml^{-1}. The time delay and wash assay therefore showed no real benefit therefore it was decided to continue with the control LFD assay with a sample volume of 50 µl as it had less steps, was less time consuming and would not require complicated microfluidic channels in the final LFD format. The authors acknowledge that this is not ideal however the complexity of multiplexing biomarkers can sometimes complicate the development process and compromises must be made.

3.2. LFD characterisation

LFD characterisation is the process of demonstrating that the LFD performance characteristics meet the requirement for the intended application and that the assay is thereby suitable for its intended use as well as applicable to real world application. Experiments that were conducted included examining LOD, single and multiplex analysis and matrix effects. Finally, real certified serum samples were also assessed in a preliminary study.

Table 1 Comparison of the characteristics of the calibration curves for different sample volumes (1–50 µl). CRP concentration was measured in µg ml^{-1} and TSH concentration measured in µIU ml^{-1}. Visual LOD was calculated as the concentration of biomarker providing a test spot signal visible by the Lumos Leelu LFD reader. LOD based on IC_{10} was calculated as the concentration providing a 10% inhibition of the signal. R^2 of curve was the goodness of fit for the 4PL curve[a]

Biomarker	Printing	Sample volume (µl)	LOD based on IC_{10}	Visual LOD	R^2 of curve
CRP	Multiplex	50	0.002	0.010	1.000
CRP	Multiplex	25	0.004	0.010	0.999
CRP	Multiplex	10	0.007	0.010	1.000
CRP	Multiplex	5	0.014	0.010	0.999
CRP	Multiplex	2.5	0.025	0.100	1.000
CRP	Multiplex	1	0.075	0.100	1.000
TSH	Multiplex	50	1.5	2.5	0.990
TSH	Multiplex	25	2.0	5	0.993
TSH	Multiplex	10	2.1	10	0.995
TSH	Multiplex	5	9.7	25	1.000
TSH	Multiplex	2.5	n.d	50	n.d
TSH	Multiplex	1	n.d	50	n.d

[a] n.d was not determinable.

Open Access Article. Published on 12 March 2026. Downloaded on 3/19/2026 3:27:56 PM.
This article is licensed under a Creative Commons Attribution-NonCommercial 3.0 Unported Licence.

3.2.1. Single and multiplex LFD analysis. In the context of a LFD, selectivity is the ability to accurately detect a specific biomarker while remaining inert to interfering substances or structural analogues. High selectivity is vital to ensure that the assay identifies only the intended target, thereby preventing false positives. This parameter is primarily governed by the antibodies integrated into the test spots and the gold-nanoparticle conjugate. These antibodies are designed to recognise unique epitopes on the target analyte. For this study, monoclonal antibodies, derived from a single B-cell clone, were utilised to ensure binding to a single, specific epitope, providing high analytical selectivity and specificity. The detection mechanism mirrors the 'lock and key' model, where the high-affinity receptors on the monoclonal antibodies ensure that only the target molecule fits the binding site. Furthermore, all LFD components and buffer formulations were refined during the optimisation phase to eliminate non-specific binding, ensuring that signal generation is strictly dependent on the presence of the target biomarker. LFDs were printed in a single system (TSH or CRP) and a two-plex system (TSH and CRP), but each system was also assessed with single and multiplex calibration standards. LFD assays were examined for single and multiplex analysis to check curve shape and to assess cross reactivity and non-specific binding for both TSH and CRP in PBS (Fig. 4). Table 2 shows the LOD based on IC_{10} and visual LOD for each system assessed for TSH and CRP. Similar curve shape and intensity (Fig. 4a) were evident for CRP for multiplex printing (with single Gold-CRP-NP and single CRP standards) and multiplex printing with multiplex Gold-NP and multiplex standards with a LOD of 0.002 μg ml^{-1} (Table 2) observed for both. Although a visual LOD of 0.01 μg ml^{-1} was detected. LOD was similar for single CRP printing (with single Gold-CRP-NP and single CRP standards) however the curve shape was slightly shifted (Fig. 4a). Similar curve shape and intensity (Fig. 4b) was evident for TSH for single TSH printing (with single Gold-TSH-NP and single TSH standards) and multiplex printing (with single Gold-TSH-NP and single TSH standards) with a LOD of 1.2 and 1.7 μIU ml^{-1} achieved respectively. Slight suppression of intensity was observed for multiplex printing (with multiplex Gold-NP and multiplex standards) with a corresponding loss in LOD to 2.7 μIU ml^{-1} for TSH. This highlighted that multiplexing had a significant effect for TSH. This loss of sensitivity for TSH was deemed acceptable for this application as our aim was to diagnose hypothyroidism at a clinical level of 5 μIU ml^{-1}. A decrease in sensitivity can be common when multiplexing, however, most importantly non-specific binding and cross reactivity between biomarkers was not observed for either TSH or CRP.

3.2.2. Matrix effects. LFD assays were examined to determine the difference in curve shape and sensitivity between PBS

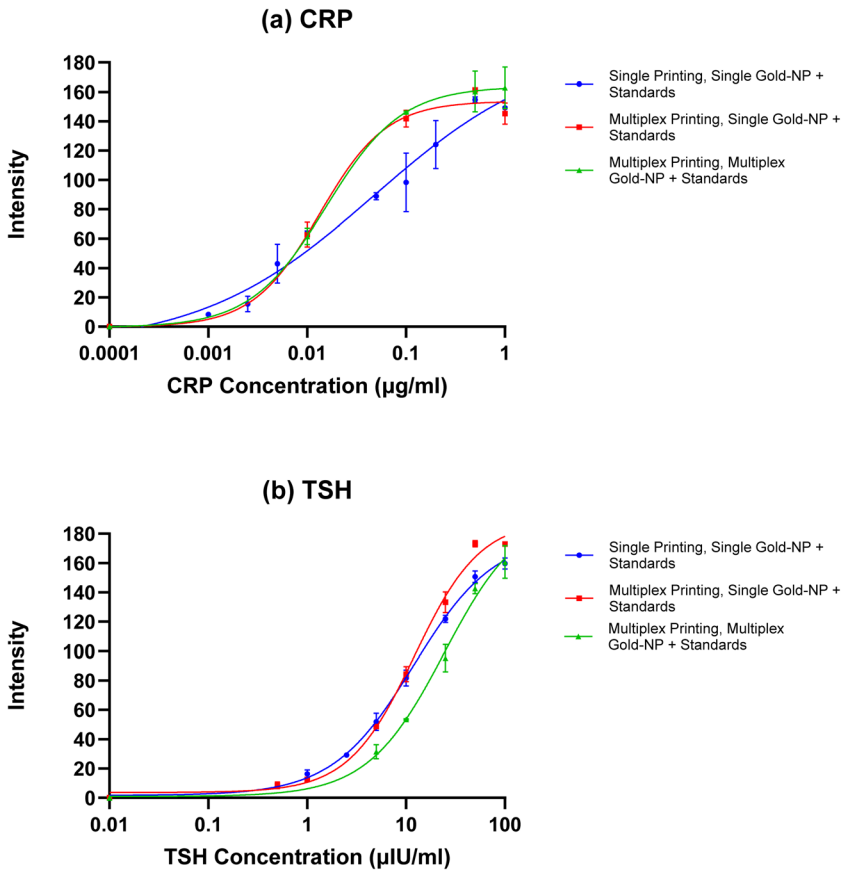

Fig. 4 Single and multiplex calibration curves in PBS for (a) CRP and (b) TSH incorporating single and multiplex printing and single and multiplex Gold-NP and standards for a full evaluation ($n = 2$ LFDs, $n = 3$ spots per LFD).

 © 2026 The Author(s). Published by the Royal Society of Chemistry

Open Access Article. Published on 12 March 2026. Downloaded on 3/19/2026 3:27:56 PM.
This article is licensed under a Creative Commons Attribution-NonCommercial 3.0 Unported Licence.

Table 2 Comparison of the characteristics of the calibration curves for single and multiplex LFD systems. CRP concentration was measured in μg ml^{-1} and TSH concentration measured in μIU ml^{-1}. Visual LOD was calculated as the concentration of biomarker providing a test spot signal visible by the Lumos Leelu LFD reader. LOD based on IC_{10} was calculated as the concentration providing a 10% inhibition of the signal. R^2 of curve was the goodness of fit for the 4PL curve

Biomarker	Printing	Gold-NP and standards	LOD based on IC_{10}	Visual LOD	R^2 of curve
CRP	Single	Single	0.001	0.001	0.981
CRP	Multiplex	Single	0.002	0.010	0.992
CRP	Multiplex	Multiplex	0.002	0.010	1.000
TSH	Single	Single	1.2	0.5	0.999
TSH	Multiplex	Single	1.7	0.5	0.996
TSH	Multiplex	Multiplex	2.7	5	0.996

and serum for a full evaluation of matrix effects for TSH and CRP (Fig. 5). Table 3 shows the LOD based on IC_{10} and visual LOD for each system assessed for TSH and CRP. Unfortunately, serum free from both TSH and CRP could not be sourced therefore single calibration curves were performed in the corresponding biomarker free serum. A serum purchased was customised for our application but still contained very low levels of both analytes when tested and interfered with analysis and therefore, could not be used. TSH free serum contained very low levels of CRP and CRP free serum contained very low levels of TSH. Therefore, multiplex analysis could not be performed as hoped. Instead, single serum calibration curves in the corresponding biomarker free serum were performed. In addition, multiplex analysis was performed in CRP free serum (that contained very low levels of TSH) and a correction factor was utilised. The average intensity of the spots for the zero-calibration standard for TSH was calculated and this intensity was subtracted from each of the other calibration standards as a correction factor. In addition, multiplex analysis was performed in CRP free serum (containing very low levels of TSH). A solution was to calculate the intensity of the spots for the zero-calibration standard and subtract intensity away from each of the other calibration standards as a correction factor. This was not ideal, but the authors hope that by showing both single serum curves in their respective analyte free serum and multiplex analysis in CRP free serum (and including correction factor for TSH) that this should be enough to show proof of concept for the multiplex LFD assay. For CRP different curve shapes (Fig. 5a) were evident between PBS and serum with serum showing a small suppression in intensity with a LOD of 0.004 μg ml^{-1} was observed in PBS compared to 0.007 μg ml^{-1} in serum. In contrast, for TSH there was a difference in curve shape between PBS and serum with serum showing an enhancement

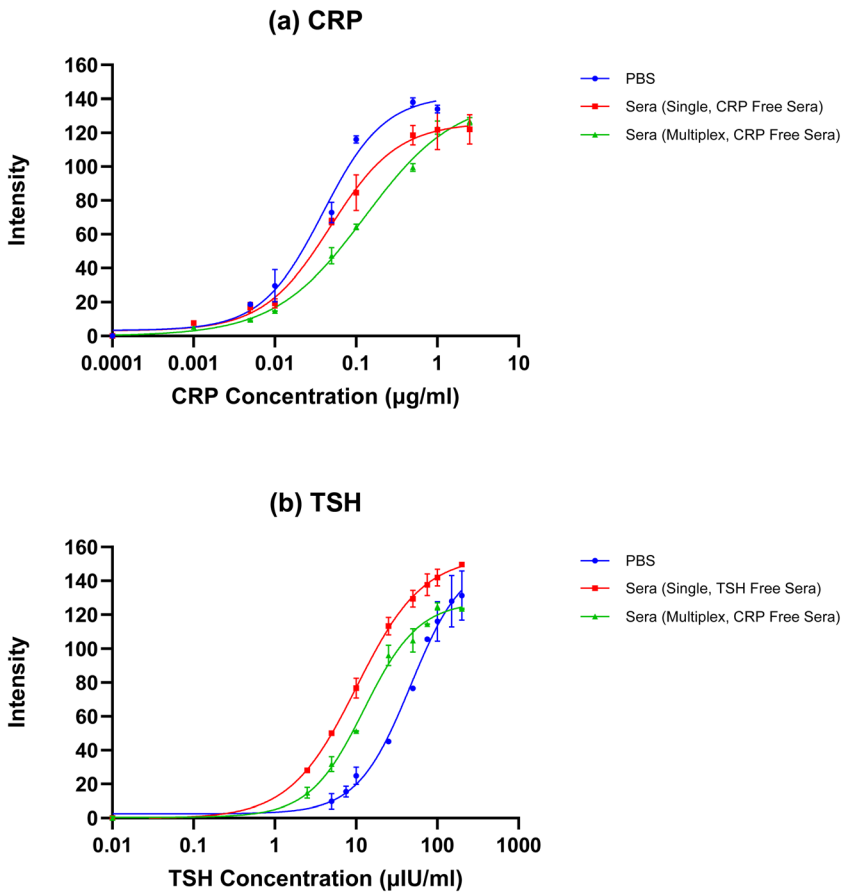

Fig. 5 Comparison of matrix effects for serum for (a) CRP and (b) TSH using the multiplex LFD (n = 2 LFDs, n = 3 spots per LFD).

Open Access Article. Published on 12 March 2026. Downloaded on 3/19/2026 3:27:56 PM.
This article is licensed under a Creative Commons Attribution-NonCommercial 3.0 Unported Licence.

Table 3 Comparison of the characteristics of the calibration curves for matrix effects. CRP concentration was measured in μg ml^{-1} and TSH concentration measured in μIU ml^{-1}. Visual LOD was calculated as the concentration of biomarker providing a test spot signal visible by the Lumos Leelu LFD reader. LOD based on IC_{10} was calculated as the concentration providing a 10% inhibition of the signal. R^2 of curve was the goodness of fit for the 4PL curve

Biomarker	System	Matrix	LOD based on IC_{10}	Visual LOD	R^2 of curve
CRP	Multiplex	PBS	0.004	0.005	0.988
CRP	Single	Sera (CRP free sera)	0.004	0.001	0.997
CRP	Multiplex	Sera (CRP free sera)	0.007	0.001	0.996
TSH	Multiplex	PBS	6.6	5	0.996
TSH	Single	Sera (TSH free sera)	1.2	2.5	1.000
TSH	Multiplex	Sera (CRP free sera)	2.1	2.5	0.995

in intensity compared to PBS (Fig. 5b). This enhancement led to an improvement in LOD for TSH to 2.1 μIU ml^{-1} which was evident in the multiplex serum curves compared to 6.6 μIU ml^{-1} in PBS. The significant difference between PBS and serum calibration curves for TSH and CRP meant that the analysis of serum samples would need to be carried out with a matrix matched serum calibration curve to ensure accurate determination of biomarker concentrations and to maintain minimal matrix effects. This highlights the importance of moving onto the proper matrix as soon as possible during LFD development.

3.3. Analysis of clinical serum samples

The analysis of certified serum samples ($n = 17$) using the multiplex LFD are presented in Table 4. These samples included TSH negative ($n = 1$), TSH positive ($n = 12$) and CRP positive ($n = 4$) serum samples. Certified serum samples were read from a single serum calibration curve due to issues sourcing a TSH and CRP free serum. The sample concentrations for the certified samples were determined from a 4PL fit calibration curve. Percentage recovery was calculated based on the concentration obtained from the multiplex LFD and that detailed by the supplier. All positive samples ($n = 16$) analysed met 60–130% recovery with 12 samples meeting 70–130% recovery. No false negative or false positive results were reported for the multiplex LFD therefore the multiplex LFD shows promise as an early warning screening method for the potential diagnosis of hypothyroidism and the potential risk of the development of coronary heart disease in those patients.

4. Conclusion

In summary, a multiplex LFD has been developed for the quantitative and simultaneous screening of two biomarkers for the diagnosis of hypothyroidism. It meets the clinical specifications (5 μIU ml^{-1}) for hypothyroidism with a LOD of 2.1 μIU ml^{-1} for TSH. Monitoring programmes for these biomarkers have become a necessity because of the potential dangers to human health. The simplicity and sensitivity achieved with the multiplex LFD means it could be used as an early warning monitoring tool for the potential diagnosis of hypothyroidism and the potential risk of the development of coronary heart disease in those patients. This technology demonstrates the feasibility as a portable, rapid, easy to use, multi biomarker detection and is a major advancement in the field of POC diagnostics. This study has demonstrated the proof of concept of a multiplex LFD for two biomarkers with results available after 30 min for immediate treatment plans or further investigations. The benefit of this multiplex LFD system is that it follows established LFD protocols, whereby laboratories with immunological screening methods already in place have end users familiar with the steps of the analysis. Also, due to COVID the public are also now familiar with how to operate and interpret LFDs. While microarray LFDs are established in food safety and emerging in biomedicine, this study introduces what

Table 4 Certified serum samples analysis ($n = 17$). Samples were assessed by the multiplex LFD, images were read by the Lumos Leelu LFD reader and images processed manually using ImageJ. Serum samples included TSH negative ($n = 1$), TSH positive ($n = 12$) and CRP positive ($n = 4$). Serum samples were assessed singly but read from a duplicate serum calibration curve. Certified samples were read from a single serum calibration curve due to issues sourcing a TSH and CRP free serum. The sample concentrations for the certified samples were determined from a 4PL fit calibration curve and results were compared to those obtained by the supplier. CRP concentration was measured in μg ml^{-1} and TSH concentration measured in μIU ml^{-1}[a]

Sample	Biomarker	Supplier concentration	Multiplex LFD concentration	Recovery (%)
1	TSH	0.04	0.1	n/a
2	TSH	23.2	16.7	72
3	TSH	22.7	15.0	66
4	TSH	18.4	16.5	90
5	TSH	16.0	18.4	115
6	TSH	11.1	7.1	64
7	TSH	10.7	7.0	65
8	TSH	9.0	9.6	107
9	TSH	8.9	9.0	101
10	TSH	7.7	7.1	93
11	TSH	6.7	8.4	125
12	TSH	5.6	4.3	77
13	TSH	3.0	1.9	63
14	CRP	3	3.5	116
15	CRP	26	19.3	74
16	CRP	24	25.6	107
17	CRP	3	2.9	98

[a] n/a = not applicable.

 © 2026 The Author(s). Published by the Royal Society of Chemistry

Open Access Article. Published on 12 March 2026. Downloaded on 3/19/2026 3:27:56 PM.
This article is licensed under a Creative Commons Attribution-NonCommercial 3.0 Unported Licence.

is, to our knowledge, the first multiplexed LFD specifically for thyroid health and hypothyroidism. Despite the clinical necessity, no commercial multiplexed LFD is currently available for thyroid health, with existing POC solutions typically limited to single-analyte TSH screening. As the shift toward personalised medicine accelerates, there is a demand for diagnostics that can simultaneously monitor multiple biomarkers. This microarray based platform represents a significant advancement in POC diagnostics, offering a scalable, multi-target solution that aligns with the future of individualised thyroid management. This study has shown some very promising data worthy of further research to determine if this approach is suitable for a commercial diagnostic test in the biomedical industry. Improvements to the sensitivity for TSH would allow the dual diagnosis of hypothyroidism and hyperthyroidism. The addition of other biomarkers to the LFD *e.g.*, T3 and T4 would be extremely beneficial in determining overall thyroid health. Stability testing of the multiplex LFD would be important before commercialisation. Additionally, prior to implementation a full validation (including intra and inter reproducibility) and an interlaboratory trial of the multiplex LFD should be conducted following accreditation guidelines. The technologies adaptability for a field study in hospitals, GP clinics and home testing are also areas of interest. To evaluate multiplexing performance, this study utilised a commercial Lumos Leelu LFD reader for image acquisition. A key future direction of this research is the development of a fully integrated, all-in-one POC system for thyroid health. This comprehensive platform will incorporate the multiplex LFD, a dedicated reader and custom image analysis software with a patient interface, enabling the simultaneous detection of multiple biomarkers for the screening of hypothyroidism and potentially thyroid function. Spotted microarray LFDs create low-cost, multiplexed POC diagnostic tools that offer a path toward decentralised medicine, however, several critical challenges and evolving perspectives shape their future. Key challenges include maintaining sensitivity and specificity. Furthermore, the simultaneous optimisation of multiple analytes is complicated by the differing binding affinities of various antibody pairs. Finally, ensuring data reproducibility remains a hurdle due to the precision required in spotting techniques, inherent batch-to-batch variability and the complex interference found in real-world sample matrices. Future perspectives for spotted microarray LFDs include the transition toward decentralised, personalised medicine in home settings, alongside the integration of artificial intelligence and smartphone-based data analysis. Furthermore, the adoption of novel sample matrices, such as saliva, offers a path toward significantly less invasive diagnostic testing.

Conflicts of interest

There are no conflicts of interest to declare.

Data availability

Data used in this study will be made available upon request from the corresponding author.

Acknowledgements

This project was funded by the Randox Centre for Excellence for Biomedical Applications (Ref. No. 059RDEN-2) and Invest Northern Ireland.

References

1 F. Hou, S. Sun, S. W. Abdullah, Y. Tang, X. Li and H. Guo, *Anal. Methods*, 2023, **15**, 2154–2218.
2 A. I Khan, M. Khan and R. Khan, *Ann. Lab. Med.*, 2023, **43**, 401–407.
3 G. Xing, J. Ai, N. Wang and Q. Pu, *Trends Anal. Chem.*, 2022, **157**, 116792.
4 J. Park, *Sensors*, 2022, **22**, 7398.
5 M. Pohanka, *Int. J. Anal. Chem.*, 2021, **202**, 1–9.
6 K. Wang, W. Qin, Y. Hou, K. Xiao and W. Yan, *Nano Biomed. Eng.*, 2016, **8**, 172–183.
7 M. Sajid, A. Kawde and M. Daud, *J. Saudi Chem. Soc.*, 2015, **19**, 689–705.
8 C. Beri and K. Pablo, *Microfluid. Nanofluid.*, 2016, **20**, 104.
9 X. Zhao, Y. Zhang, Q. Niu, L. Wang, C. Xing, Q. Wang and H. Bao, *Sensors*, 2024, **24**, 1989.
10 L. Zhan, S. Guo, F. Song, Y. Gong, F. Xu, D. R. Boulware, M. C. McAlpine, W. C. W. Chan and J. C. Bischof, *Nano Lett.*, 2017, **17**, 7207–7212.
11 A. Sena-Torralba, R. Álvarez-Diduk, C. Parolo, A. Piper and A. Merkoçi, *Chem. Rev.*, 2022, **122**(18), 14881–14910.
12 D. Gasperino, T. Baughman, H. V. Hsieh, D. Bell and B. H. Weigl, *Annu. Rev. Anal. Chem.*, 2018, **11**, 219–244.
13 L. Anfossi, F. Di Nardo, S. Cavalera, C. Giovannoli and C. Baggiani, *Biosens*, 2018, **9**, 2.
14 C. Dincer, R. Bruch, A. Kling, P. S. Dittrich and G. A. Urban, *Trends Biotechnol.*, 2017, **35**, 728–742.
15 K. M. Hanafiah, N. Arifin, Y. Bustami, R. Noordin, M. Garcia and D. Anderson, *Diagnostics*, 2017, **7**, 51.
16 J. Li and J. Macdonald, *Biosens. Bioelectron.*, 2016, **83**, 177–192.
17 S. K. Bikkarolla, S. E. McNamee, P. Vance and J. McLaughlin, *Biosens*, 2022, **12**, 182.
18 K. Kim, D. K. Han, N. Choi, S. H. Kim, Y. Joung, K. Kim, N. T. Ho, S. Joo and J. Choo, *Anal. Chem.*, 2021, **93**, 6673–6681.
19 S. K. Bikkarolla, S. E. McNamee, S. McGregor, P. Vance, H. McGhee, E. L. Marlow and J. McLaughlin, *AIP Adv.*, 2020, **10**, 125316.
20 S. L. Znoyko, A. V. Orlova, V. A Bragina, M. P. Nikitin and P. I. Nikitin, *Talanta*, 2020, **216**, 120961.
21 L. Khelifa, Y. Hu, N. Jiang and A. K. Yetisen, *Lab Chip*, 2022, **22**, 2451–2475.
22 P. Ridker, *Inflammation, Tex. Heart Inst. J.*, 2005, **32**, 3.
23 M. Pohanka, *Biosens.*, 2022, **12**, 344.
24 J. Oh, H. Joung, H. S. Han, J. K. Kim and M. Kim, *Theranostics*, 2018, **8**, 3189–3197.
25 I. N. Katis, P. J. W. He, R. W. Eason and C. L. Sones, *Biosens. Bioelectron.*, 2018, **113**, 95–100.

Open Access Article. Published on 12 March 2026. Downloaded on 3/19/2026 3:27:56 PM.
This article is licensed under a Creative Commons Attribution-NonCommercial 3.0 Unported Licence.

26 E. G. Rey, D. O'Dell, S. Mehta and D. Erickson, *Anal. Chem.*, 2017, **89**, 5095–5100.
27 Y. K. Oh, H. Joung, H. S. Han, H. Suk and M. Kim, *Biosens. Bioelectron.*, 2014, **61**, 285–289.
28 W. Leung, C. P. Chan, T. H. Rainer, M. Ip, G. W. H. Cautherley and R. Renneberg, *J. Immunol. Methods*, 2008, **336**, 30–36.
29 M. Christ-Crain, M. Guglielmetti, P. R. Huber, W. Riesen, J. Staub and B. Muller, *Atherosclerosis*, 2003, **166**, 379–386.
30 A. Tuzcu, M. Bahceci, D. Gokalp, Y. Tuzun and K. Gunes, *Endocr. J.*, 2005, **52**, 89–94.
31 T. Nagasaki, M. Inaba, K. Shirakawa, Y. Hiura, H. Tahara, Y. Kumeda, T. Ishikawa, E. Ishimura and Y. Nishizawa, *Biomed. Pharmacother.*, 2007, **61**, 167–172.
32 E. Savas, A. Z. Sahin, S. N. Aksoy, A. Tascan, Z. A. Sayıner and M. Ozkaya, *Int. J. Cl in. Exp. Med.*, 2016, **9**, 4485–4490.
33 N. Ahmad, S. Nagtilak, A. K. Sharma and P. Parashar, *JMSCR*, 2018, **6**, 485–489.
34 C. Tang, Y. Dong, L. Lu and N. Zhang, *Endocr. Connect.*, 2021, **10**, 965–972.

 © 2026 The Author(s). Published by the Royal Society of Chemistry